7686 *Biochemistry* **2009,** *48,* 7686–7697
DOI: 10.1021/bi900795a

BIOCHEMISTRY
including biophysical chemistry & molecular biology
Article

Two Secondary Carbohydrate Binding Sites on the Surface of Barley α-Amylase 1 Have Distinct Functions and Display Synergy in Hydrolysis of Starch Granules[†]

Morten M. Nielsen,[‡] Sophie Bozonnet,[‡,§] Eun-Seong Seo,[‡] János A. Mótyán,[∥] Joakim M. Andersen,[‡] Adiphol Dilokpimol,[‡] Maher Abou Hachem,[‡] Gyöngyi Gyémánt,[∥] Henrik Næsted,[‡] Lili Kandra,[∥] Bent W. Sigurskjold,[⊥] and Birte Svensson*[,‡,§]

[‡]*Enzyme and Protein Chemistry, Department of Systems Biology, Technical University of Denmark, Søltofts Plads, Building 224, DK-2800 Kgs. Lyngby, Denmark,* [§]*Carlsberg Laboratory, Gamle Carlsberg Vej 10, DK-2500 Copenhagen Valby, Denmark,* [∥]*Department of Biochemistry, Faculty of Sciences, University of Debrecen, Debrecen, Hungary H-4010, and* [⊥]*Department of Biology, University of Copenhagen, DK-2100 Copenhagen Ø, Denmark*

Received May 8, 2009; Revised Manuscript Received July 14, 2009

ABSTRACT: Some polysaccharide processing enzymes possess secondary carbohydrate binding sites situated on the surface far from the active site. In barley α-amylase 1 (AMY1), two such sites, SBS1 and SBS2, are found on the catalytic $(\beta/\alpha)_8$-barrel and the noncatalytic C-terminal domain, respectively. Site-directed mutagenesis of Trp^{278} and Trp^{279}, stacking onto adjacent ligand glucosyl residues at SBS1, and of Tyr^{380} and His^{395}, making numerous ligand contacts at SBS2, suggested that SBS1 and SBS2 act synergistically in degradation of starch granules. While SBS1 makes the major contribution to binding and hydrolysis of starch granules, SBS2 exhibits a higher affinity for the starch mimic β-cyclodextrin. Compared to that of wild-type AMY1, the K_d of starch granule binding by the SBS1 W278A, W279A, and W278A/W279A mutants thus increased 15−35 times; furthermore, the k_{cat}/K_m of W278A/W279A was 2%, whereas both affinity and activity for Y380A at SBS2 were 10% of the wild-type values. Dual site double and triple SBS1/SBS2 substitutions eliminated binding to starch granules, and the k_{cat}/K_m of W278A/W279A/Y380A AMY1 was only 0.4% of the wild-type value. Surface plasmon resonance analysis of mutants showed that β-cyclodextrin binds to SBS2 and SBS1 with $K_{d,1}$ and $K_{d,2}$ values of 0.07 and 1.40 mM, respectively. A model that accounts for the observed synergy in starch hydrolysis, where SBS1 and SBS2 bind ordered and free α-glucan chains, respectively, thus targeting the enzyme to single α-glucan chains accessible for hydrolysis, is proposed. SBS1 and SBS2 also influence the kinetics of hydrolysis for amylose and maltooligosaccharides, the degree of multiple attack on amylose, and subsite binding energies.

Several starch-degrading enzymes of glycoside hydrolase (GH) families 13, 14, 15, and 77 from bacteria (*1*−*6*), archaea (*7*), fungi (*8*, *9*), mammals (*10*−*13*), and plants (*14*, *15*) (http://www.cazy.org/) contain secondary carbohydrate binding sites situated on the surface a certain distance from the catalytic site and substrate binding cleft. Barley α-amylase 1 (AMY1)[1] of GH13, catalyzing hydrolysis of 1,4-α-D-glucosidic linkages in starch and related poly- and oligosaccharides, has two such surface binding sites called "the starch granule-binding surface site" (*14*) and "the pair of sugar tongs" (*15*−*19*), here termed SBS1 and SBS2, respectively. The substrate maltoheptaose and the substrate analogues methyl $4^I,4^{II},4^{III}$-trithiomaltotetraoside (thio-DP4) and acarbose are accommodated at the active site and surface sites in crystal structures of wild-type AMY1 and the isozyme AMY2 (sequence 80% identical to that of AMY1), as well as in AMY1 catalytic nucleophile and SBS2 mutants (*15*, *17*, *18*, *20*). SBS1 is exposed on the side of the catalytic $(\beta/\alpha)_8$-barrel domain, while SBS2 is observed on the C-terminal antiparallel β-sheet domain (*15*, *20*). Noticeably, as it is very common in protein−carbohydrate interactions, aromatic side chains are central in binding at SBS1 and SBS2 (*14*, *15*, *17*−*19*). Mutations at the substrate binding active site cleft have previously demonstrated the potential for engineering the relative specificity for oligosaccharides versus polysaccharides, including manipulation of subsite binding energy profiles and the degree of multiple attacks on amylose (*21*−*25*). This study emphasizes an emerging understanding of the functional roles of secondary binding sites in amylolytic enzymes as well as in other polysaccharide processing enzymes.

[†]This work was supported by the Danish Natural Science Research Council, the Danish Research Council for Technology and Production Sciences, the Carlsberg Foundation, the Danish Centre for Advanced Food Studies (LMC), the OTKA T047075 grant from the Hungarian Scientific Research Fund (to L.K.), the EU fifth Framework Program to Project CEGLYC (QLK3-CT-2001-00149), an H. C. Ørsted postdoctoral fellowship from the Technical University of Denmark and a fellowship from the Korean Government (MOEHRD) (KRF-2005-214-D0075) (both to E.-S.S.), and a Ph.D. scholarship from the Technical University of Denmark (to M.M.N.).

*To whom correspondence should be addressed: Enzyme and Protein Chemistry, Department of Systems Biology, Technical University of Denmark, Søltofts Plads, Building 224, DK-2800 Kgs. Lyngby, Denmark. Phone: +45 4525 2740. Fax: +45 4588 6307. E-mail: bis@bio.dtu.dk.

[1]Abbreviations: AMY1 and AMY2, barley α-amylase 1 and 2, respectively; β-CD, β-cyclodextrin; BCF, bond cleavage frequency; Bl-pNP-G7, 4,6-*O*-benzylidine-modified 4-nitrophenyl β-D-maltoheptaoside; CBM, carbohydrate binding module; CGTase, cyclodextrin glucanotransferase; Cl-pNP-G7, 2-chloro-4-nitrophenyl β-D-maltoheptaoside; CNP-MOS, 2-chloro-4-nitrophenyl β-D-maltooligosaccharides; DMA, degree of multiple attack; DP, degree of polymerization; GH13, glycoside hydrolase family 13; iBS, insoluble Blue Starch; RU, response unit; SBD, starch binding domain; SBS1 and SBS2, surface binding site 1 and 2, respectively; SPR, surface plasmon resonance; SUMA, SUbsite Mapping of Amylases, a program for apparent binding energy calculation; thio-DP4, methyl $4^I,4^{II},4^{III}$-trithiomaltotetraoside.

 Published on Web 07/16/2009

Barley α-amylase SBS1 and SBS2 are not recognized in other α-amylases or related enzymes. Carbohydrate binding sites different from SBS2 are seen in the C-terminal domains of α-amylases from *Bacillus halmapalus* and *Aspergillus niger*, but these were not further investigated (*6*, *9*). Recently, in human salivary α-amylase, several aromatic residues identified at four secondary binding sites were substituted in various combinations by alanine and concluded to be involved in binding and hydrolysis of raw as well as soluble starch and noticeably also in activity toward maltopentaose and maltoheptaose (*13*). A surface binding site on the catalytic domain of the *Neisseria polysaccharea* amylosucrase from GH13 was described, on the basis of mutational analysis and molecular modeling, to capture and direct the growing α-glucan chain for elongation at the acceptor binding area of the active site (*26*, *27*). By contrast, no function was yet proposed for a carbohydrate binding site situated on the C-terminal domain of the same enzyme (*26*, *27*). Finally, in certain starch-metabolizing enzymes, including a few α-amylases, different secondary binding sites are encountered on individual starch binding domains (SBDs), i.e., carbohydrate binding modules (CBMs) (http://www.cazy.org/) (*28*, *29*) placed N- or C-terminally of the catalytic domain and connected by separate globular domains or polypeptide linkers (*29*−*31*). However, there is no overall structural resemblance between the α-amylase C-terminal domain consisting of an antiparallel β-sheet and the β-sandwich fold adopted by SBDs. This does not preclude functional or architectural similarities which may be evolutionarily driven for the molecular recognition of the same substrate.

SBS1 in AMY1 and AMY2 is a carbohydrate binding platform formed by Trp^{278} and Trp^{279} (Trp^{276} and Trp^{277} in AMY2), which are stabilized by several surrounding residues. The indole rings of these two residues stack onto two adjacent glucosyl units in different ligands (*14*, *17*, *18*). A couple of decades ago, β-cyclodextrin (β-CD) was demonstrated to protect these tryptophanyl residues in AMY2 against chemical modification (*32*). This finding guided site-directed mutagenesis in the AMY1 isozyme, as production of recombinant AMY2 was extremely inefficient (*33*). Only W279A AMY1, however, was obtained using *Saccharomyces cerevisiae* as a host and in a very poor yield of ∼100 μg from a 150 L culture, which limited characterization of this first surface site mutant of a polysaccharide-degrading enzyme to merely a confirmation of its role in affinity for starch granules and β-CD (*34*). SBS2, seen in AMY1, has a prominent Tyr^{380} making eight of a total of 17 interactions with thio-DP4 accompanied by a 3.1 Å shift of the Tyr^{380} side chain (*15*). His^{395} that flanks the shallow cavity forming SBS2 on the opposite side of Tyr^{380} contributes with only two ligand contacts and has a minor impact on the enzymatic properties of AMY1 (*16*). The Y380A and Y380M AMY1 mutants, however, were found to cause an ∼10-fold loss in affinity for β-CD and starch granules. This underscores the functional importance of Tyr^{380} and thus confers a key role to domain C in a GH13 member (*17*). Remarkably, a site in AMY2 structures that corresponds to SBS2 in AMY1 did not accommodate ligands even though Tyr^{380} and His^{395} are conserved (Tyr^{378} and His^{393} in AMY2) and the C-terminal domains of AMY1 and AMY2 superimpose very well (*14*, *19*).

Since high-resolution structures are not available to illustrate molecular interactions of enzymes and polysaccharide substrates, characterization of surface binding site mutants can provide insight into the importance of multiple binding sites in enzymatic processing of polysaccharides. The use of this strategy takes advantage of efficient production of wild-type recombinant AMY1 and mutants by *Pichia pastoris* (*33*) enabling mutational analysis of structure−function relationships of the two secondary carbohydrate binding sites, SBS1 and SBS2.

MATERIALS AND METHODS

Strains, Plasmids, and Site-Directed Mutagenesis. *Escherichia coli* DH5α (Invitrogen, Carlsbad, CA) and XL10-Gold ultracompetent cells (Stratagene, La Jolla, CA) and *P. pastoris* X-33 (Invitrogen) were used for cloning and heterologous expression, respectively. pPICZA-AMY1 encoding AMY1Δ9 with a C-terminal nonapeptide truncation (*23*), hereafter termed AMY1, and pPICZA-AMY1 Y380A (*17*) were in-house stocks. Standard cloning techniques were used (*35*). pPICZA-AMY1, W278A, W279A, and W278A/W279A were prepared (QuickChange XL site-directed mutagenesis kit; Stratagene) using a W278A sense primer [5′-CCCGGCGTGATGGGAGCTTGGCCGGCCAAGGCCGTCACC-3′ (mutant codon underlined)], a W278A antisense primer (5′-GGTGACGGCCTTGGCCGGCCAAGCTCCCATCACGCCGGG-3′), a W279A sense primer (5′-CCCGGCGTGATGGGATGGCTCCGGCCAAGGCCGTCACC-3′), a W279A antisense primer (5′-GGTGACGGCCTTGGCCGGAGCCCATCCCATCACGCCGGG-3′), a W278A/W279A sense primer (5′-CCCGGCGTGATGGGAGCTGCTCCGGCCAAGGCCGTCACC-3′), and a W278A/W279A antisense primer (5′-GGTGACGGCCTTGGCCGGAGCAGCTCCCATCACGCCGGG-3′) with pPICZA-AMY1 as the template. The resulting pPICZA-AMY1 mutants were digested with *Nsi*I, and DNA fragments encoding W278A, W279A, and W278A/W279A were subcloned in pPICZA-AMY1 Y380A. Plasmids were propagated in *E. coli* DH5α or XL10-Gold ultracompetent cells (low-salt LB, 25 μg/mL Zeocin), purified (HiSpeed Plasmid Midi Kit, Qiagen, Germantown, MD), sequenced (Big-Dye premix; ABI PRISM 310 Genetic Analyzer, Perkin-Elmer Life Sciences, Waltham, MA), linearized with *Pme*I, transformed in *P. pastoris* by electroporation (*33*), selected on YPDS plates [1% (w/v) yeast extract, 2% (w/v) peptone, 2% (w/v) glucose, 1 M sorbitol, 2% (w/v) agar, and 100 μg/mL Zeocin], and screened for α-amylase secretion on MM-starch plates [1.34% (w/v) yeast nitrogen base, 4×10^{-5}% (w/v) biotin, 0.5% (v/v) methanol, and 2% (w/v) soluble potato starch] by being exposed to I_2 (*23*, *36*).

Protein Expression and Purification. Transformants were grown (0.8 L of BMGY, 30 °C, 48 h in 3 L flasks) to an OD_{600} of ∼15 (*17*), using BMM [100 mM potassium phosphate (pH 6.0), 1% (w/v) casamino acids, 1.34% (w/v) YNB, 4 μg/mL biotin, and 0.5% (v/v) methanol] for induction. α-Amylase activity was assayed toward insoluble Blue Starch (iBS) and used to calculate the yield of secreted enzymes. Cell harvest and induction were repeated two or three times, and the combined supernatants were centrifuged and concentrated to ∼150 mL (10 kDa cutoff, Pellicon, Millipore Corp., Billerica, MA) (*17*) and the enzymes purified either by affinity chromatography on β-CD-Sepharose [AMY1 W278A, W279A, and W278A/W279A (*17*, *21*, *36*)] or by anion exchange chromatography on ResourceQ (6 mL) using gradient elution (AKTAexplorer, GE Healthcare, Uppsala, Sweden) [AMY1 W278A/Y380A, W279A/Y380A, and W278A/W279A/Y380A (*17*)]. Eluate containing α-amylase, detected by iBS assay and SDS−PAGE (NuPage 4−12% Bis-Tris, Invitrogen), was concentrated to ∼1 mg/mL (Centriprep, 10 kDa cutoff, Millipore), dialyzed [10 mM MES (pH 6.8) and 25 mM $CaCl_2$], added 0.02% (w/v) NaN_3, and kept at 4 °C. Y105A (*21*),

Y105A/Y380A, H395A, and Y380A/H395A AMY1 (*16*) were in-house stocks.

Enzyme Activity Assays. (*i*) *Insoluble Blue Starch* (*iBS*). The activity of α-amylase (1−12 nM) was measured toward iBS (6.25 mg/mL customer preparation, Pharmacia) at 37 °C in 25 mM sodium acetate (pH 5.5), 5 mM $CaCl_2$, and 0.005% (w/v) BSA. One unit corresponds to the amount of enzyme that yields a ΔOD_{620} of 1 (*17*, *23*). (*ii*) *Amylose*. Hydrolysis of amylose DP (degree of polymerization) 440 (potato type III, Sigma, St. Louis, MO) was assessed as described previously (*17*, *23*) after addition of enzyme (0.8−1.6 nM) at 10 substrate concentrations (0.1−2.5 mg/mL) in 20 mM sodium acetate (pH 5.5), 5 mM $CaCl_2$, 0.005% (w/v) BSA, and 4% DMSO at 37 °C. k_{cat} and K_m were calculated by fitting the Michaelis−Menten equation to the initial rates (GraphPad Prism version 3.02, GraphPad Software, San Diego, CA) (*17*). (*iii*) *2-Chloro-4-nitrophenyl β-D-Maltoheptaoside*. After enzyme (25−60 nM) was added, the rate of hydrolysis at eight concentrations (0.25−10 mM) of Cl-pNP-G7 (Sigma) was followed as described previously (*17*) at A_{405} in 50 mM sodium phosphate (pH 6.8), 50 mM KCl, 0.005% (w/v) BSA, and 0.02% (w/v) NaN_3 at 30 °C using 2-chloro-4-nitrophenol as the standard. k_{cat} and K_m were calculated as described above. (*iv*) *4,6-O-Benzylidine-Modified 4-Nitrophenyl β-D-Maltoheptaoside*. Hydrolysis of Bl-pNP-G7 (Megazyme, Bray, Ireland) was followed essentially as described for Cl-pNP-G7 (*17*) except that 4-nitrophenol (Sigma) was used as the standard. (*v*) *Starch Granules*. After enzyme (6−60 nM) was added, release of soluble reducing sugar from barley starch granules (Primalco) suspended at 10 concentrations (0.8−400 mg/mL) in 20 mM sodium acetate (pH 5.5), 5 mM $CaCl_2$, and 0.005% (w/v) BSA was followed during a 25 min incubation with agitation (1000 rpm) at 37 °C as measured in supernatants after centrifugation (16000*g* for 15 min) (*17*). k_{cat} and K_m were calculated for the wild type from initial rates as described above, while for mutants, the catalytic coefficient k_{cat}/K_m was obtained from the slope of v_i/[E] versus [S].

Subsite Mapping. 2-Chloro-4-nitrophenyl β-D-maltooligosaccharides (CNP-MOS) of DP 3−11 were in-house stocks (*37*, *38*), and action patterns were determined as reported previously (*25*) for 1 mM CNP-MOS in 20 mM sodium acetate and 5 mM $CaCl_2$ (pH 5.5) at 37 °C with added enzyme (0.2−1000 nM) by monitoring CNP-glucoside and CNP-MOS release (at 302 nm) at time intervals using HPLC (ZORBAX Eclipse XDB-C18 column, 5 μm, 4.6 mm × 150 mm, 10 μL aliquots) eluted with an acetonitrile/water mixture (13/87, 1 mL/min) at 40 °C (Hewlett-Packard 1090 Series II liquid chromatograph, diode array detector, autosampler, and ChemStation). Products increased linearly and maintained their distribution for at least 20 min. Bond cleavage frequencies (BCFs) were calculated for individual glucosidic linkages in CNP-MOS relative to all bond cleavages at <10% substrate conversion to minimize the influence of product hydrolysis. SUMA (SUbsite Mapping for α-Amylases) using BCFs was used to calculate the number of subsites, the catalytic site position, and individual subsite affinities (exempting subsites −1 and +1 that are occupied in all productive complexes). Apparent free energy values were optimized by minimization of differences between experimental and calculated BCFs (*39*).

Degree of Multiple Attack (*DMA*). Enzyme (0.1−2.0 nM) was added to 1 mg/mL amylose DP440 in 20 mM sodium acetate (pH 5.5), 5 mM $CaCl_2$, 0.005% BSA, and 2% (v/v) DMSO, and the initial rates of release of reducing power in the total digest (RV_t) and in the polysaccharide fraction precipitated by ethanol (RV_p) were measured using copper bicinchoninate with maltose as the standard (*22*). DMA was calculated according to eq 1. Experiments were conducted in at least triplicate.

$$\mathrm{DMA} = \frac{\mathrm{RV_t}}{\mathrm{RV_p}} - 1 \quad (1)$$

Carbohydrate Binding. (*i*) *Starch Granules*. Enzyme (5−10 nM) and barley starch granules (Primalco) at 14 concentrations (0.1−40 and 0.5−100 mg/mL for enzyme variants showing wild-type and weak affinity levels, respectively) in 20 mM sodium acetate (pH 5.5), 5 mM $CaCl_2$, and 0.005% (w/v) BSA were incubated in triplicate at 4 °C for 30 min with end-over-end mixing and centrifuged (16000*g* and 4 °C for 5 min) (*17*). Supernatants were transferred to Eppendorf tubes on ice and assayed for activity toward iBS. The dissociation constant K_d was obtained by fitting the Langmuir adsorption isotherm to the fraction of bound enzyme (eq 2)

$$B = \frac{B_{max}[S]}{K_d + [S]} \quad (2)$$

B being the bound enzyme fraction, [S] the starch granule concentration, and B_{max} the maximum binding capacity. The effect of β-CD on starch granule binding was studied in parallel. (*ii*) *β-Cyclodextrin*. The K_d for β-CD binding was determined with the aid of surface plasmon resonance (SPR) analysis (BIAcore 3000; Biacore International AB, Uppsala, Sweden) using streptavidin-coated sensor chips charged with 2000−3000 response units (RU) of biotinylated enzyme. Biotinylation of W278A, W279A, and W278A/W279A AMY1 was performed essentially as reported previously (*17*, *40*) in 9 mM β-CD, 10 mM MES (pH 6.8), 25 mM $CaCl_2$, and 0.02% (w/v) NaN_3. Sensorgrams (RU vs time) were recorded at 25 °C for 12 β-CD concentrations (15 μM to 7 mM) in running buffer [10 mM MES (pH 6.5), 5 mM $CaCl_2$, and 0.005% (v/v) surfactant P20] at a rate of 30 μL/min for 3 min followed by a 3 min dissociation in running buffer and baseline-corrected by subtracting data from parallel flow cells with no enzyme. The equilibrium dissociation constant K_d was calculated by steady state affinity fitting (eq 3) using BIAevaluation version 3.1 (BIAcore)

$$R = \frac{R_{max}[\beta\text{-CD}]}{[\beta\text{-CD}] + K_d} \quad (3)$$

R being the response, [β-CD] the β-CD concentration, and R_{max} the maximum binding capacity. Analyses were conducted in triplicate (*17*). A model assuming two independent binding sites (eq 4) (GraphPad Prism version 3.02 as described above) where R, [β-CD], $K_{d,1}$, $K_{d,2}$, $R_{max,1}$, and $R_{max,2}$ are defined as for eq 3 above was fitted to data for enzymes biotinylated in the presence of β-CD.

$$R = \frac{R_{max,1}[\beta\text{-CD}]}{[\beta\text{-CD}] + K_{d,1}} + \frac{R_{max,2}[\beta\text{-CD}]}{[\beta\text{-CD}] + K_{d,2}} \quad (4)$$

Differential Scanning Calorimetry. W278A/W279A/Y380A and wild-type AMY1 were dialyzed against 10 mM HEPES and 0.5 mM $CaCl_2$ (pH 7.5) and analyzed at 5.1 and 4.7 μM, respectively, using a differential scanning calorimeter (MicroCal, Northhampton, MA; cell volume of 0.5072 mL) at a scan rate of 60 °C/h. All solutions were degassed by being stirred under vacuum. Scans of dialysate were subtracted as references

from sample scans. Data were analyzed using Origin version 7.0 supplied with the calorimeter. The midpoint temperature T_m was determined corresponding to the maximum C_p (*41*).

Molecular Graphics and Sequence Alignments. D180A AMY1/maltoheptaose (Protein Data Bank entry 1RP8) (*18*) was used for structure-based evaluation of mutations using PyMOL (http://www.pymol.org) for molecular model rendering. Sequence segments from selected plant α-amylases covering SBS1 and SBS2 were aligned using Vector NTI Advance version 10.3 (Invitrogen). Alignment rendering was done with ESPript (*42*).

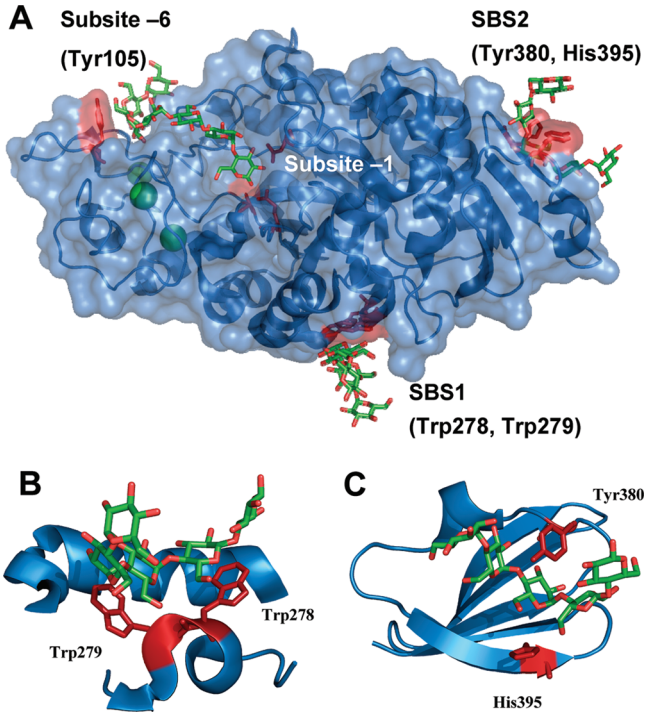

FIGURE 1: (A) Overall structure of the maltoheptaose complex with the inactive catalytic nucleophile mutant D180A AMY1 [Protein Data Bank entry 1RP8 (*18*)]. Calcium ions are shown as green spheres. Maltoheptaose in the active site cleft is represented by sticks, and the three catalytic residues, Glu^{205}, Asp^{291}, and the D180A mutation are colored red. In the bottom part of the figure, five sugar rings of maltoheptaose bound at SBS1 via stacking interaction with Trp^{278} and Trp^{279} can be seen (red). In domain C (to the right), five sugar rings of maltoheptaose fixed between Tyr^{380} and His^{395} (red) from SBS2 can be seen. Close-ups of (B) SBS1 and (C) SBS2.

RESULTS

Choice and Production of Surface Site Mutants. The roles of key carbohydrate-interacting aromatic residues at SBS1 and SBS2 in AMY1 (Figure 1) were investigated using alanine substitution. The dual site SBS1/SBS2 mutants W278A/Y380A, W279A/Y380A, and W278A/W279A/Y380A AMY1 were compared with the SBS1 (Figure 1B) W278A, W279A, and W278A/W279A mutants and the SBS2 (Figure 1C) Y380A mutant to discern the contribution of pivotal aromatic residues to the properties of the two binding sites and to gain insight into their possible synergy or cooperativity. The previously characterized AMY1 variants Y105A (*21*), Y105A/Y380M, Y380A, H395A, and Y380A/H395A (*16*) involving SBS2 as well as the high-affinity substrate binding −6 subsite of the active site cleft were included in this analysis of the impact of surface sites on the subsite map, i.e., the profile of substrate binding energies along subsites −8 through +4 in the active site.

The host *P. pastoris* secreted recombinant wild-type AMY1 at a level of 40−60 mg/L (*33*), and the surface site variants were successfully produced, albeit in 2−8-fold lower yields, which is common for AMY1 mutants (*16*, *17*, *23*, *24*). The triple mutant W278A/W279A/Y380A AMY1 was produced at only 1 mg/L, even though the DSC thermograms of wild-type AMY1 and the triple mutant (not shown) were essentially the same, having unfolding temperatures, T_m, of 80 and 78.6 °C, respectively, indicating preserved structural integrity upon surface site mutations. Therefore, altered activity and binding properties found after substitutions at SBS1 and SBS2 were attributed to local changes in ligand interactions rather than to loss of the overall enzyme folding.

Enzymatic Activity. The various surface site mutations influenced enzymatic activity differently, but the trend was similar for changes in k_{cat} on the soluble substrates and the specific activity toward iBS (Table 1). Thus, the k_{cat} values toward amylose and maltoheptaoside of W278A/W279A at SBS1, Y380A at SBS2, and the three dual site SBS1/SBS2 variants represented modest decreases to 17−70 and 32−68% of the wild-type values, respectively (Table 1), whereas mutation

Table 1: Enzymatic Activities toward Insoluble Blue Starch, Amylose DP440, and 2-Chloro-4-nitrophenyl β-D-Maltoheptaoside or 4,6-*O*-Benzylidine-Modified 4-Nitrophenyl β-D-Maltoheptaoside

	iBS[a]	amylose DP440[b]			Cl-pNP-G7[c] or Bl-pNP-G7		
AMY1	specific activity (units/mg)	k_{cat} (s^{-1})	K_m (mg/mL)	k_{cat}/K_m (s^{-1} mg^{-1} mL) (%)	k_{cat} (s^{-1})	K_m (mM)	k_{cat}/K_m (s^{-1} mM^{-1}) (%)
wild-type	2800	169 ± 8	0.13 ± 0.01	1300 (100)	36 ± 3 132 ± 8[e]	0.7 ± 0.1 0.71 ± 0.02[e]	48 (100) 185 (100)
W278A	2600	196 ± 47	0.27 ± 0.02	726 (56)	40 ± 1	0.7 ± 0.2	57 (120)
W279A	2415	170 ± 19	0.24 ± 0.05	708 (54)	38.5 ± 0.7	0.53 ± 0.04	72 (150)
W278A/W279A	1080	48 ± 2	0.34 ± 0.03	141 (11)	79 ± 3[e]	0.83 ± 0.05[e]	95 (51)
Y380A[d]	1400	95 ± 15	0.36 ± 0.02	264 (20)	19.0 ± 0.6	0.67 ± 0.05	28 (58)
W278A/Y380A	1800	91 ± 3	0.30 ± 0.02	303 (23)	73 ± 2[e]	0.76 ± 0.08[e]	96 (52)
W279A/Y380A	2000	119 ± 16	0.34 ± 0.03	350 (27)	90 ± 1[e]	0.81 ± 0.04[e]	112 (61)
W278A/W279A/Y380A	589	30 ± 1	0.56 ± 0.05	54 (5.0)	43 ± 2[e]	1.4 ± 0.2[e]	31 (17)

[a] The rate at 6.25 mg/mL iBS in 25 mM sodium acetate (pH 5.5), 5 mM $CaCl_2$, and 0.005% (w/v) BSA. [b] Rates were determined at 10 concentrations (0.1−2.5 mg/mL) of amylose DP440 in 20 mM sodium acetate (pH 5.5), 5 mM $CaCl_2$, 0.005% (w/v) BSA, and 4% (v/v) DMSO. [c] Rates were determined at eight concentrations (0.25−10 mM) of Cl-pNPG$_7$ in 50 mM sodium phosphate (pH 6.8), 50 mM KCl, 0.005% (w/v) BSA, and 0.02% (w/v) NaN_3. The standard deviation was calculated from triplicate experiments. [d] Data from ref *17*. [e] Bl-pNP-G7 as the substrate.

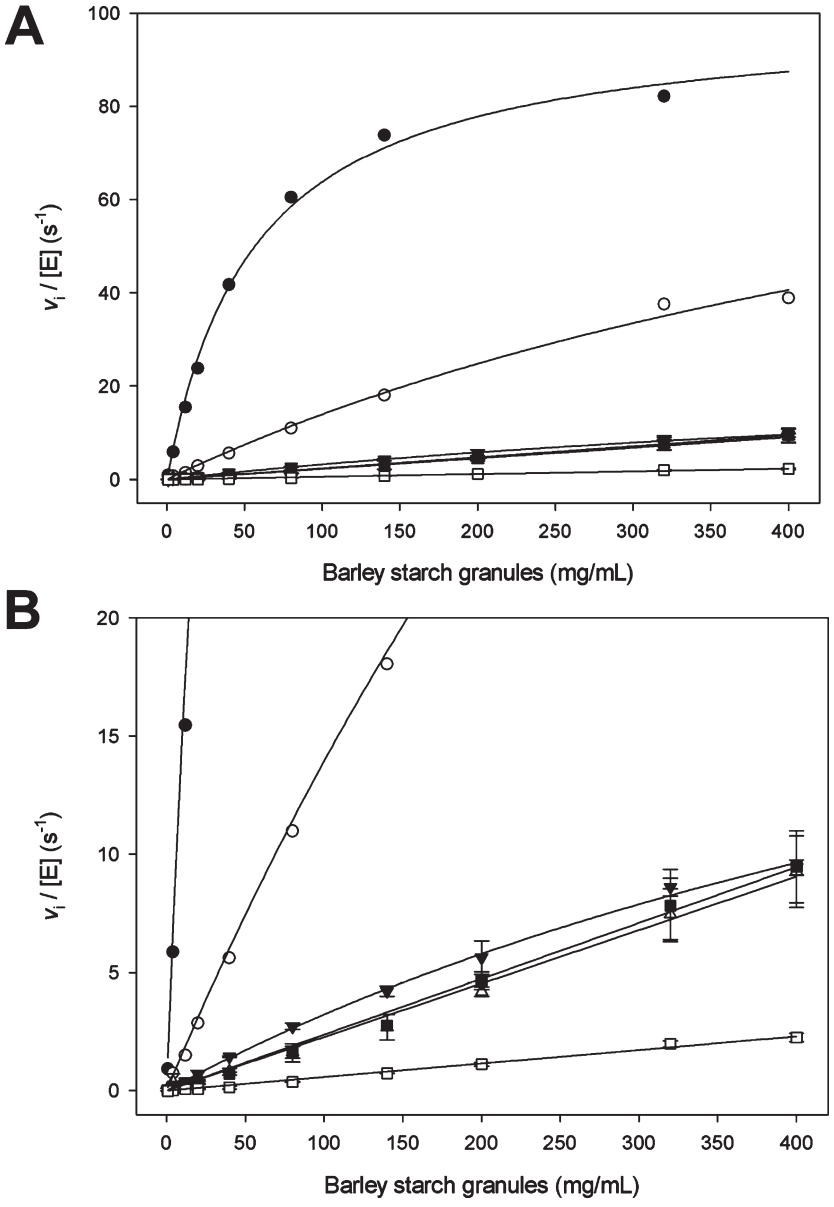

FIGURE 2: Hydrolysis of barley starch granules by SBS1 and SBS2 mutants. (A) The release of soluble reducing products is shown as a function of the concentration of barley starch granules: (●) AMY1, (○) Y380A, (▼) W278A/W279A, (△) W278A/Y380A, (■) W279A/Y380A, and (□) W278A/W279A/Y380A. (B) Close-up of curves of W278A/W279A and the dual starch binding site mutants (▼) W278A/W279A, (△) W278A/Y380A, (■) W279A/Y380A, and (□) W278A/W279A/Y380A.

of only one of the two SBS1 residues in W278A and W279A AMY1 did not affect the k_{cat} values and the specific activity, although it doubled K_m toward amylose (Table 1). The W278A/W279A/Y380A mutant gave the largest (4-fold) increase in K_m toward amylose and was the sole variant to exhibit a small increase (i.e., a doubling) in K_m for maltoheptaoside (Table 1).

Degradation of Barley Starch Granules. AMY1 and AMY2 are very important in the mobilization of storage starch to oligosaccharides that supply the growing plantlet during germination of barley seeds. AMY1 catalyzed degradation of suspended barley starch granules followed Michaelis−Menten kinetics (Figure 2A) with an apparent K_m of 73 mg/mL and a k_{cat} of 113 s^{-1}. The two surface sites showed no apparent cooperativity since the curve was nonsigmoidal and the Hill coefficient, n, was found to be 1. In the case of all surface site mutants, only the catalytic efficiency, k_{cat}/K_m, and not the individual k_{cat} and K_m values could be determined, because of weakened binding (Figure 2B). While the SBS1 and dual site SBS1/SBS2 mutants W278A/W279A, W278A/Y380A, and W279A/Y380A retained ~2%, the triple variant W278A/W279A/Y380A AMY1 retained only 0.4% of the wild-type activity. The k_{cat}/K_m, however, was considerably higher for the SBS2 mutant Y380A AMY1 and corresponded to 10% of the wild-type value (Table 2).

Degree of Multiple Attack (DMA). Hydrolysis of amylose DP440 by AMY1 was previously found to proceed according to a multiple-attack mechanism, and the quantitative analysis of oligosaccharide product profiles indicated that the polysaccharide substrate interacted with the enzyme surface at a site situated outside of the active site region (*22*). Wild-type AMY1 shows a DMA value of ~2 (*22*), on amylose, which means that after the initial endo attack, two more glucosidic bonds are hydrolyzed during the same enzyme−substrate encounter (*22*). A loss of one of these second events in the mutants W278A/W279A and W278A/W279A/Y380A AMY1 was inferred from their DMA values of 1.1 and 1.2, respectively, and was similar to the loss previously measured for the SBS2 Y380A mutant (*17*) (Table 3).

The reduction of the DMA of W278A and W279A to 1.3 and 1.6, respectively, furthermore indicated that both SBS1 tryptophans participate in the multiple attack. Overall, SBS1 and SBS2 appeared essentially equally important, but they were not found to cooperate in the multiple-attack mechanism, since once one site was impaired the abolition of the other did not further suppress the DMA.

Mapping of Active Site Subsite Binding Energies. Certain surface site mutations altered the oligosaccharide product profiles from CNP-MOS of DP3−11, reflecting apparent differences in the energies of binding or repulsion of substrate glucosyl residues at subsites −8 through +4 of the active site. Most remarkably, the calculated subsite maps of SBS2 mutants Y380A and H395A revealed a striking gain and a striking loss in the total subsite binding energy determined to be −39.7 and −12.6 kJ/mol, respectively, compared to the wild-type AMY1 value of −22.6 kJ/mol (Table 4). The binding energy gain in Y380A was fairly evenly distributed along the active site subsites and accompanied by a noteworthy conversion of one internal and two external repulsive (positive energy values) barrier subsites −5, −8, and +4 in wild-type AMY1 (*25*) to binding (negative energy values) subsites in the variant (Table 4). In contrast, H395A flanking the opposite edge of the SBS2 binding cavity (Figure 1C) caused a distinct loss of affinity due to strengthened repulsion at several barrier subsites and a weaker affinity for the two most important binding subsites, −6 and −2. The SBS2 Y380A/H395A mutant gave intermediate subsite binding affinities of the Y380A and H395A mutants (Table 4), a behavior possibly reminiscent of the activity differences for Y380A/H395A, Y380A, and H395A AMY1, with the double mutant surprisingly showing activity superior to that of each of its constituent single mutants (*16*). Subsite maps of SBS1 and dual site SBS1/SBS2 W279A, W278A/Y380A, and W279A/Y380A mutants resembled that of the wild type without the affinity gain characteristic of the Y380A mutant (Table 4). Finally, the previously demonstrated dominant role of Tyr^{105}, which is in direct contact with the substrate at the most favorable binding subsite −6 (*16*) over Tyr^{380} in activity toward oligosaccharides, was evident from Y105A and Y105A/Y380M AMY1, both of which were undergoing a large reduction of ∼7 kJ/mol of the 12.4 kJ/mol affinity at subsite −6 in the wild type (Table 4).

Binding to Starch Granules. Mutations at SBS1 and SBS2 greatly impaired the affinity of AMY1 for barley starch granules. The single W278A and W279A mutants thus had 15-fold larger K_d values than the wild type, and the K_d of the double mutant W278A/W279A AMY1 was 35-fold increased and revealed that Trp^{278} and Trp^{279} each contributed cumulatively to ensure optimal binding to the natural substrate (Table 5). The role of SBS1 was further illustrated by the 19−24% reduction in the starch saturation binding level B_{max} for the mutants. By contrast, the SBS2 mutants Y380A, H395A, and Y380A/H395A resulted in just 2−11-fold increased K_d values (*16*).

No binding was detected toward starch granules for all three dual site W278A/Y380A, W279A/Y380A, and W278A/W279A/Y380A mutants. Hence, although SBS1 clearly provided the major contribution to the affinity for starch granules, the optimal binding depended on both SBS1 and SBS2. When the starch mimic β-CD was added to compete with binding to starch granules, the apparent K_d was largely increased for the two SBS1 single mutants and was too weak to be measured for the

Table 2: Rates of Hydrolysis of Barley Starch Granules by AMY1 Surface Site Mutants

AMY1	k_{cat}/K_m (s^{-1} mg mL^{-1})	ratio (wild-type:mutant) (k_{cat}/K_m:k_{cat}/K_m)
wild-type[a]	1.549	1.0
W278A	0.129	12.0
W279A	0.177	8.7
W278A/W279A	0.035	51.6
Y380A[b]	0.151	10.2
W278A/Y380A	0.023 ± 0.003	67.3
W279A/Y380A	0.024 ± 0.004	64.5
W278A/W279A/Y380A	0.0059 ± 0.0004	263

[a] k_{cat} = 113 ± 12 s^{-1}, and K_m = 73 ± 15 mg/mL (this work). [b] Data from ref *17*.

Table 3: Degrees of Multiple Attack (DMA) by AMY1 Mutants on Amylose DP440[a]

AMY1	RV_t (s^{-1})	RV_p (s^{-1})	DMA (RV_t/RV_p − 1)
wild-type	108 ± 13	38 ± 4	1.9 ± 0.2
W278A	91 ± 4	40 ± 2	1.3 ± 0.1
W279A	124 ± 8	48 ± 3	1.6 ± 0.1
W278A/W279A	64 ± 3	31 ± 2	1.1 ± 0.1
W278A/W279A/Y380A	16 ± 1	7.2 ± 0.6	1.2 ± 0.2
Y380A[b]	53 ± 5	25 ± 5	1.1 ± 0.2

[a] See ref *22* and Materials and Methods for details. [b] Data from ref *17*. The analyses were performed in triplicate.

Table 4: Mapping of Individual Active Site Subsite Binding Energies of AMY1 Mutated at SBS1, SBS2, and Subsite −6[a]

	binding energy[b] calculated for subsites −8 through +4 (kJ/mol)												
AMY1	−8	−7	−6	−5	−4	−3	−2	−1	+1	+2	+3	+4	total binding energy (kJ/mol)
wild-type[c]	0.3	−4.0	−12.4	0.8	−1.3	1.0	−7.0	−	−	−2.7	1.9	0.8	−22.6
W279A	0.2	−3.9	−10.0	−0.2	−1.9	0.7	−4.6	−	−	−3.0	2.3	−1.1	−21.5
W278A/Y380A	0.4	−3.0	−10.6	2.9	−1.1	0.9	−5.1	−	−	−2.7	2.4	0.3	−15.6
W279A/Y380A	0.6	−3.9	−11.7	1.7	−0.8	0.8	−5.7	−	−	−2.7	2.3	0.0	−19.4
Y380A	−1.0	−6.9	−14.0	−1.9	−2.7	0.2	−8.7	−	−	−5.4	2.0	−1.3	−39.7
H395A	1.3	−3.8	−8.0	2.6	−0.5	0.9	−5.5	−	−	−2.7	2.9	0.2	−12.6
Y380A/H395A	0.8	−4.3	−10.7	0.1	−0.7	0.5	−5.8	−	−	−2.5	2.4	−0.2	−20.4
Y105A[c]	0.7	−3.8	−5.6	0.2	−1.4	0.2	−8.0	−	−	−5.0	2.0	0.9	−19.8
Y105A/Y380M	0.2	−3.8	−5.4	0.2	−1.6	−0.6	−7.6	−	−	−4.8	1.6	0.0	−21.8

[a] See Materials and Methods for details. [b] Negative and positive values indicate binding and repulsion, respectively. Differences in energy values calculated from BCFs of parallel measurements are < 0.6 kJ/mol. [c] Data from ref *25*.

Table 5: Binding of AMY1 SBS1 and SBS2 Variants to Barley Starch Granules[a]

			added β-CD[c]	
AMY1	K_d (mg/mL)	B_{max}	K_d (mg/mL)	B_{max}
wild-type	0.64 ± 0.06	0.98 ± 0.02	2.9 ± 0.3	0.98 ± 0.02
W278A	9.7 ± 0.9	0.81 ± 0.03	81 ± 10	0.76 ± 0.08
W279A	11 ± 2	0.82 ± 0.04	77 ± 37	0.78 ± 0.13
W278A/W279A	22 ± 2	0.76 ± 0.01	> 100	~0.40
Y380A[b]	5.9 ± 0.5	0.90 ± 0.05	6.9 ± 0.6	0.81 ± 0.02

[a] No binding to barley starch granules was observed for W278A/Y380A, W279A/Y380A, or W278A/W279A/Y380A. [b] Data from ref *17*. [c] Binding was assessed in the presence of 0.5 mM β-CD.

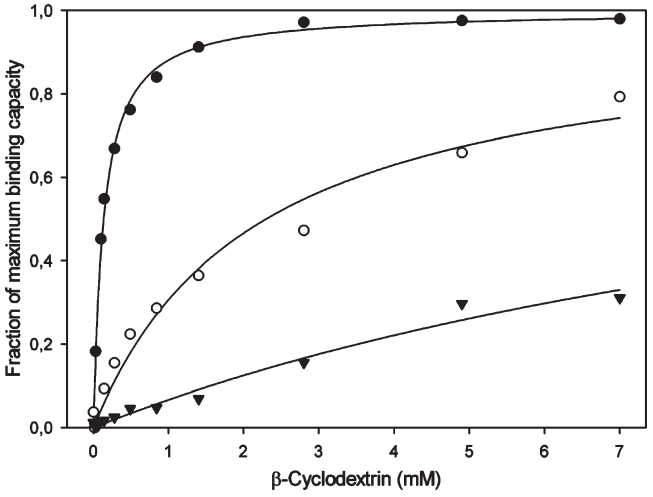

FIGURE 3: SPR analysis of β-CD binding to AMY1. The fraction of maximum binding capacity is plotted as a function of β-CD concentration: (●) AMY1, (○) Y380A, and (▼) W278A/W279A/Y380A.

SBS1 double mutant, whereas the K_d value of the Y380A mutant, which has SBS1 intact, was only marginally increased (Table 5).

β-Cyclodextrin Binding. The AMY1−β-CD complex (Figure 3) was formed according to a model with two distinct binding sites giving the best fit to the SPR sensorgrams (Table 6). By SPR analysis of single site mutants, a stronger binding event and a weaker binding event with a $K_{d,1}$ of 0.07 mM and a $K_{d,2}$ of 1.4 mM were assigned to SBS2 and SBS1, respectively (Table 6). A Scatchard plot confirmed the presence of two β-CD binding sites (Figure 4A) that differed in affinity by ~20-fold. Fitting of the Hill equation to the SPR RU data versus β-CD concentration gave a Hill coefficient (n) of ~1, indicating that SBS1 and SBS2 did not cooperate in β-CD binding (Figure 4B). The very high K_d value for W278A/W279A/Y380A AMY1 estimated to be > 7 mM may reflect either highly reduced residual affinity at one or both of the mutated surface sites or recognition of the oligosaccharide at a very weak binding site detected only when the SBS1 and SBS2 sites were destroyed (Table 6). Both possibilities agree with a $K_{d,2}$ of > 7 mM found for SBS1 mutants (Table 6). The dominant role of SBS2 in β-CD binding is seen in both dual site W278A/Y380A and W279A/Y380A mutants having similarly reduced affinity for β-CD versus that of the single Y380A SBS2 mutant (Table 6).

Table 6: Binding of β-Cyclodextrin to AMY1 SBS1 and SBS2 Mutants

	one-site binding	two-site binding	
AMY1	K_d[c] (mM)	$K_{d,1}$[d] (mM)	$K_{d,2}$[d] (mM)
wild-type[a]	na[e]	0.07 ± 0.01	1.44 ± 0.31
W278A[a]	na[e]	0.08 ± 0.01	> 7.0
W279A[a]	na[e]	0.076 ± 0.005	−
W278A/W279A[a]	na[e]	0.08 ± 0.01	> 7.0
Y380A[b]	1.40 ± 0.23	na[e]	na[e]
W278A/Y380A	0.89 ± 0.16	na[e]	na[e]
W279A/Y380A	1.42 ± 0.14	na[e]	na[e]
W278A/W279A/Y380A[a]	> 7.0	−	−

[a] The enzyme was biotinylated in the presence of β-CD, and data were fitted to a two-site model (see Materials and Methods). [b] Data from ref *17*. [c] K_d determined using a one-site binding model. [d] $K_{d,1}$ and $K_{d,2}$ determined using a two-site binding model (see Materials and Methods). [e] Model not applicable.

DISCUSSION

Enzymatic polysaccharide degradation becomes enigmatic, first since the size of the substrates, often organized in supramolecular structures, vastly exceeds that of the enzymes and second because numerous possibilities exist for interaction between the substrate and the enzyme surface. Several crystal structures of enzyme−oligosaccharide complexes, however, provide a glimpse of such interactions as witnessed by carbohydrate binding at surface sites situated a long distance from the active site in, for example, α-amylases (*11*, *13*, *18*), cellulases (*43*), agarase (*44*), and xylanases (*45*, *46*). Alternatively, degradation of insoluble starch granules or plant cell wall polysaccharides can be facilitated by CBMs known to (i) confer target recognition, (ii) increase the enzyme concentration near the substrate surface, and (iii) possibly guide a substrate chain to the active site. These CBM features afford comparison with secondary binding sites like SBS1 and SBS2 in AMY1.

Conservation of SBS1 and SBS2 in Plant α-Amylases. SBS1 is the first secondary binding site identified in a carbohydrate-active enzyme and was discovered by differential chemical modification and crystallography, which both indicated that Trp^{276} and Trp^{277} of barley AMY2 participated in carbohydrate binding (*14*, *32*). No suitable heterologous expression system was available for AMY2, and attempts to mutate the equivalent Trp^{278} and Trp^{279} residues in the AMY1 isozyme produced in *S. cerevisiae* (*34*) unfortunately only resulted in extremely small amounts of W279A AMY1, just enabling demonstration of a role of Trp^{279} in starch granule and β-CD binding; thus, neither W278A, W278A/W279A, nor SBS1 phenylalanine variants were obtained (*34*). In fact, phenylalanine and tyrosine were not observed corresponding to Trp^{278} and Trp^{279} in plant α-amylase sequences (Figure 5A). Remarkably, although the two tryptophans seemed to be critical for the function, the conformational stability of W278A/W279A/Y380A and wild-type AMY1 was found to be essentially the same. With regard to SBS2, structural superimposition of domain C from AMY1 and other α-amylases suggested that SBS2 is unique for plant α-amylases (*15*). A methionine in α-amylases from various beans matched AMY1 Tyr^{380}, whereas phenylalanine or tryptophan was not reported at this position (Figure 5B). Adzuki bean α-amylase binds 35 times more weakly than AMY1 to starch granules, and the mimicking Y380M AMY1 had ~10-fold lower affinity compared to that of the wild type (*16*, *17*). This affinity was further decreased by oxidation to methionine sulfoxide (*47*). The fact that no AMY2 structure contained a ligand at SBS2 (*14*), although the key AMY1 residues Tyr^{380} and His^{395} are conserved in AMY2, suggests that subtle differences in structural and presumably physicochemical properties, e.g., surface charge distribution,

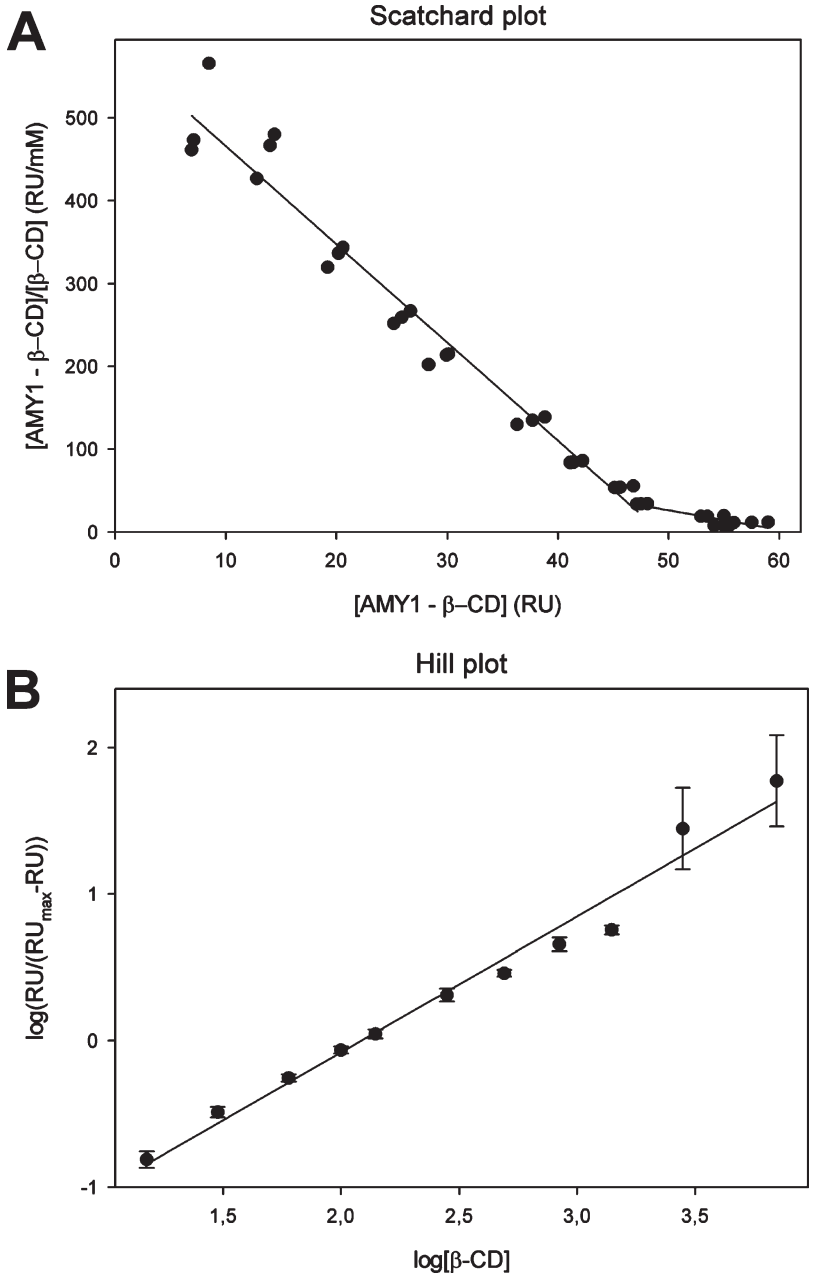

FIGURE 4: Scatchard (A) and Hill (B) plots of the SPR analysis of β-CD binding to wild-type AMY1.

distinguished AMY1 and AMY2, although such specific differences could not be pointed out (*19*). This difference may contribute to the synergy in the action of the two isozymes *in vivo* with relevance for the mobilization of starch granules that appears to be initiated by AMY1.

Impact of SBS1 and SBS2 on Enzymatic Activity toward Amylose and Maltooligosaccharides. Mutations in SBS1 and SBS2 caused modest changes in the kinetic parameters toward maltoheptaoside, indicating that binding at the active site was hardly affected by structural changes at the two distant surface sites except for a doubling of the apparent K_m and a 3-fold reduction in k_{cat} toward maltoheptaoside for the triple mutant. Similarly, a small decrease in k_{cat} was previously found for the SBS2 Y380A mutant (*17*); thus, a major role of SBS1 and SBS2 in catalytic efficiency toward maltoheptaoside was precluded. The three maltoheptaose molecules accommodated at the active site, SBS1, and SBS2 in the AMY1 D180A−maltoheptaose crystal structure (Figure 1A) are ~40 Å apart (*18*), and this distance also rationalizes the modest effect of mutations on the hydrolysis of maltoheptaoside, which has a length of roughly 38 Å assuming a linear conformation. Examination of the structure, however, does not provide a clear explanation for why the catalytic efficiency on maltooligosaccharides should vary at all due to mutations at sites distal to the active site cleft. This may be due to a requirement found earlier in kinetic studies of occupation of a secondary binding site outside of the active site for optimal activity (*48*), which may be corrupted by the surface site mutation. Another possible rationale may be that intact surface binding sites bind oligosaccharides and thus maintain a locally higher substrate concentration at the enzyme surface, resulting in an apparent increase in the Michaelis−Menten constants when these sites are abolished. This is in line with the 2-fold elevated K_m for the dual site mutant on maltoheptaoside, and it is also consistent with the apparent modest changes in the subsite energies calculated for the mutants using oligosaccharide substrates (Table 4). To this end, the remarkable gain in subsite

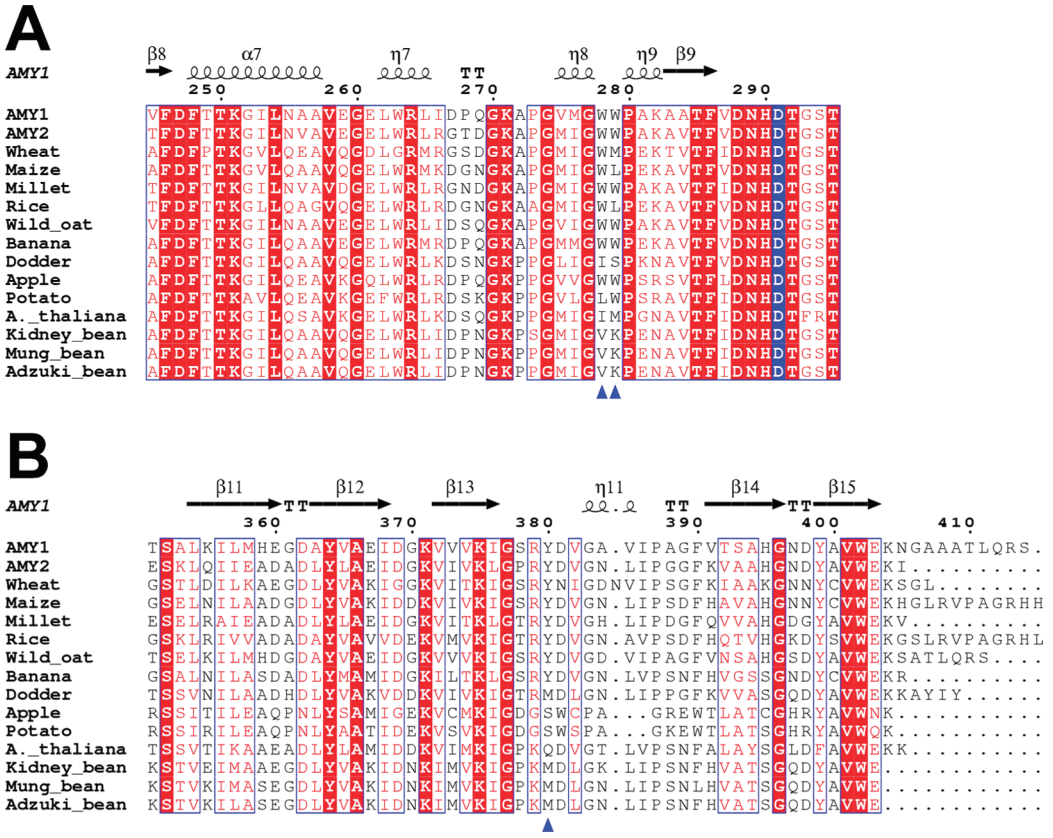

FIGURE 5: Alignments of putative (A) SBS1 and (B) SBS2 site sequences in GH13_6 α-amylases from plants (AMY1 numbering) (*56*). The secondary structure of AMY1 is marked above the alignment. Arrowheads indicate the mutated positions (W278, W279A, and Y380), and the highly conserved catalytic residue D291 is marked with a white character in a blue box. Identical residues in the alignment are marked with red boxes and white characters; similar residues are denoted with red characters, while a blue frame indicates similarity across groups. Accession numbers are as follows: P00693 for AMY1, P04063 for AMY2, P08117 for wheat (AMY3), Q41770 for maize, Q7Y1C3 for millet, P27933 for rice (AMY3), CAA09324 for wild oat, AAO11776 for banana, AAA16513 for dodder, AAF63239 for apple, M79328 for potato, CAB36742 for *Arabidopsis thaliana*, Q9ZP43 for kidney bean, P17859 for mung bean, and BAC76729 for adzuki bean.

binding affinity of Y380A AMY1 which was not maintained in the dual site mutants W278A/Y380A and W279A/Y380A can be in keeping with other changes in enzymatic properties found for Y380A being counteracted when combining Y380A with each of the SBS1 site mutations.

In contrast, effects of mutations with amylose DP440 as the substrate were evident. Thus, all mutants gave a 2−4-fold increase in the apparent K_m (Table 1), indicating that formation of productive enzyme−substrate complexes with the longer α-glucan substrate is not only mediated by the active site cleft but also enhanced by SBS1 and SBS2. The impact of the surface sites is also clear from the roughly 2- and 3-fold decrease in the k_{cat} values of Y380A at SBS2 and the SBS1 W278A/W279A double mutant, respectively. Noticeably, conservation of either Trp^{278} or Trp^{279} at SBS1 ensured the wild-type k_{cat} toward both amylose and maltoheptaoside, but the single mutations W278A and W279A still severely affected binding to and hydrolysis of starch granules.

The behavior of secondary binding site mutants is consistent with the observed modest decrease by mutation at SBS2 in activity toward maltooligosaccharides (*17*) and the proposal made earlier that oligosaccharide interaction at a distant site was required to yield full activity toward amylose (*17*, *48*). Here the lower activity of the different surface site variants for amylose made both SBS1 and SBS2 candidates for such a remote site. Finally, the reduced DMA of SBS1 and SBS2 mutants supports the hypothesis that a binding site outside of the active site also interacts with amylose during multiple attacks, and again both surface sites are candidates for such a site.

Individual and Joint Roles of SBS1 and SBS2 in Interaction with Starch Granules. Trp^{278}, Trp^{279}, and Tyr^{380} are necessary for optimal action of AMY1 on starch granules, as the three corresponding single-alanine substitutions weakened the ability to bind onto and degrade starch granules by factors of 9−15. Combination of Y380A at SBS2 with mutation at SBS1 completely abolished detectable starch granule binding. Hence, from having almost no effect on the K_m in maltoheptaose hydrolysis, the mutations of the surface sites result in more or less additive increases in K_m toward the longer amylose and act with clear synergy in starch granule binding and hydrolysis.

Interrogating the AMY1 structure provides a rationale for the experimental observations and helps in discerning the contribution of each surface site. Thus, SBS1 is located almost at the opposite side of the substrate binding cleft, while SBS2 is roughly perpendicular to it at the edge of the longer axis of the molecule. This arrangement is reminiscent of the two binding sites present in starch binding domains belonging to CBM20 (*49*, *50*). Another striking similarity to the binding sites in CBM20 resides in the architecture of SBS1 and SBS2. Thus, SBS1 is a solvent-exposed, structurally rigid platform able to bind directly onto the surface of starch granules, and similarly to binding site 1 in *A. niger* glucoamylase CBM20 (*51*), while SBS2 features a cleft confined to accommodating single α-glucan chains resembling

binding site 2 in *A. niger* CBM20, which like SBS2 undergoes significant conformational changes upon carbohydrate binding. Furthermore, binding site 2 in *A. niger* CBM20 and SBS2 both have considerably higher affinity for oligosaccharides than binding site 1 (*52*). This parallel between surface sites in AMY1 and CBM20 suggests that efficient starch hydrolysis has driven the evolution of comparable architectural features either on a separate scaffold such as CBM20 or on the surface of AMY1.

The lower affinity of SBS1 toward oligosaccharides and its flat exposed surface make it suitable for docking onto the surface of a starch granule. This is evident from the loss of function with the large increase in K_d and drop in B_{max} of binding to granular starch for the SBS1 double mutant. The results also show that SBS1 targets a higher proportion of binding sites on starch granules than those accessible for SBS2. Binding of the double mutant in the presence of 0.5 mM β-CD, i.e., at a concentration corresponding to 7 times the K_d for SBS2, strongly suppressed binding and reduced the B_{max} beyond the reliably measured range as SBS1 was impaired by the mutation and SBS2 was blocked by β-CD. Performing the same experiment on Y380A AMY1 affected much more modestly the affinity and binding capacity, as β-CD did not outcompete interaction with intact SBS1, in agreement with its K_d of 1.4 mM. The greater impact of SBS1 on starch binding and hydrolysis despite its lower affinity for β-CD may stem either from the larger population of sites that are targeted by SBS1 because of its exposed topology or from a preferentially higher affinity of SBS1 toward ordered α-glucan chains at the starch granule surface, since the entropic penalty for binding would be smaller in that case than for binding to free β-CD or free α-glucan chains. By contrast, SBS2 is suited to bind free α-glucan chains, taking advantage of Tyr^{380} seen to move to optimize interactions with oligosaccharides in crystal structures (*15*, *18*).

In summary, the results suggest that SBS1 and SBS2 serve distinct functions, which may be rationalized by the following model: SBS1 acts as an initial docking platform for starch granules and has affinity for a large variety of different sites on the starch granule, whereas binding to SBS2 targets a much smaller population of sites due to its requirement of the presence of a free α-glucan chain. Hence, maximum affinity is only achieved where both sites are occupied according to the model. The combined effect of SBS1 and SBS2 is expected to be to direct the enzyme to locations on the starch granule where there are free α-glucan chains accessible for the catalytic site. Noticeably, the K_d for adsorption of AMY1 onto starch granules was 2 orders of magnitude lower than the K_m measured for hydrolysis, a difference that may partly stem from reduction of affinity at the higher temperature used for hydrolysis as compared to binding assays performed at 4 °C and partly from only a smaller fraction of binding sites on the starch granules being susceptible to hydrolytic attack.

Mutational Analysis of Surface Binding Sites in Other Amylolytic Enzymes. Along the same lines as found for the AMY1 variants described here, multiple mutations of surface sites in human salivary α-amylase showed 10% of wild-type activity for starch accompanied by a reduced level of adsorption to starch granules, and a remarkable loss of hydrolytic activity toward maltooligosaccharides was also reported (*13*). Thus, although AMY1 and human salivary α-amylase have quite different properties, they both possess surface binding sites that affect the action at the active site on a substrate molecule that is too small to bind simultaneously at the active site and a secondary site. Furthermore, in both enzymes, the secondary sites are critical for interaction with starch granules.

Previous mutational analysis of the two binding sites in the C-terminal SBD of CBM20 from *Bacillus subtilis* strain 251 CGTase suggested they have different functions, one site guiding the α-glucan chain to the active site on the catalytic domain and the other anchoring the enzyme to the starch granule (*53*). The mutational analysis of the CGTase, however, also showed very similar affinities for starch granules, K_d values being 15.2 and 23.9 mg/mL for each of the two sites (*53*), and noticeably, binding was 20−40-fold weaker than that by AMY1. Moreover, the CGTase has a Hill coefficient of 1.7, indicating that the two sites cooperate in binding to starch granules in contrast to AMY1 (*53*). Mutational analysis of the closely related SBD of CBM20 from *A. niger* glucoamylase, proposed to mediate accessibility to the substrate by unwinding double-helical α-glucan chains on the surface of starch granules (*54*), showed, however, that CBM20 binds oligosaccharides more strongly than AMY1 does (*51*). Even though it is tempting to suggest that the SBD and the surface sites in AMY1 share functional properties, they are clearly distinguished by the dissimilar preference for starch granules and oligosaccharides, thus illustrating the wide functional and carbohydrate binding diversity of secondary binding sites. In fact, an AMY1−SBD fusion protein containing CBM20 from *A. niger* glucoamylase resulted in a 6- and 15-fold enhanced starch granule affinity and rate of degradation, respectively (*55*), emphasizing the vast potential to improve interactions with polysaccharide substrates by multisite engineering.

CONCLUSION

Our data highlight the synergy between the two carbohydrate binding sites on the surface of AMY1 in the adsorption onto and hydrolysis of starch granules, whereas observed effects of the surface sites on soluble substrates were less pronounced. The different architecture of the two binding sites defines their individual ligand preference and affinities for various substrates. Hence, SBS1 has a greater impact on the binding and hydrolysis of starch granules, whereas SBS2 displays superior affinity toward the model substrate β-CD. Moreover, the role of surface sites in activity toward the soluble maltooligosaccharides and amylose was less certain than on insoluble starch granules, although it was still clearly demonstrated by changes in the degree of multiple attack and in subsite maps. We propose that the combined effects of the secondary binding sites in AMY1 direct the enzyme to areas of the starch granules with free α-glucan chains and possibly sequester these chains into the active site cleft for hydrolysis. This work illustrates the pivotal role of surface binding sites targeting the starch granule surface in fine-tuning the mode of binding and hydrolysis, resulting in efficient degradation of insoluble starch. This underscores the importance of surface binding sites as key players in the mechanism of action of α-amylases lacking CBMs with affinity for starch.

ACKNOWLEDGMENT

Susanne Blume and Marina Rybaltover are acknowledged for excellent technical assistance, and Ahmet Alsac is acknowledged for help with preliminary experiments on W278A and W279A AMY1. We are grateful to Phaedria St. Hilaire and Monica Palcic (Carlsberg Laboratory) for advice on surface plasmon resonance. Vibeke Barkholt and Birte Kramhøft are thanked for useful discussions.

REFERENCES

1. Knegtel, R. M. A., Strokopytov, B., Penninga, D., Faber, O. G., Rozeboom, H. J., Kalk, K. H., Dijkhuizen, L., and Dijkstra, B. W. (1995) Crystallographic studies of the interaction of cyclodextrin glycosyltransferase from *Bacillus circulans* strain-251 with natural substrates and products. *J. Biol. Chem. 270*, 29256–29264.
2. Dauter, Z., Dauter, M., Brzozowski, A. M., Christensen, S., Borchert, T. V., Beier, L., Wilson, K. S., and Davies, G. J. (1999) X-ray structure of Novamyl, the five-domain "maltogenic" α-amylase from *Bacillus stearothermophilus*: Maltose and acarbose complexes at 1.7 Å resolution. *Biochemistry 38*, 8385–8392.
3. Przylas, I., Tomoo, K., Terada, Y., Takaha, T., Fujii, K., Saenger, W., and Sträter, N. (2000) Crystal structure of amylomaltase from *Thermus aquaticus*, a glycosyltransferase catalysing the production of large cyclic glucans. *J. Mol. Biol. 296*, 873–886.
4. Brzozowski, A. M., Lawson, D. M., Turkenburg, J. P., Bisgaard-Frantzen, H., Svendsen, A., Borchert, T. V., Dauter, Z., Wilson, K. S., and Davies, G. J. (2000) Structural analysis of a chimeric bacterial α-amylase. High-resolution analysis of native and ligand complexes. *Biochemistry 39*, 9099–9107.
5. Miyake, H., Kurisu, G., Kusunoki, M., Nishimura, S., Kitamura, S., and Nitta, Y. (2003) Crystal structure of a catalytic site mutant of β-amylase from *Bacillus cereus* var. *mycoides* cocrystallized with maltopentaose. *Biochemistry 42*, 5574–5581.
6. Lyhne-Iversen, L., Hobley, T. J., Kaasgaard, S. G., and Harris, P. (2006) Structure of *Bacillus halmapalus* α-amylase crystallized with and without the substrate analogue acarbose and maltose. *Acta Crystallogr. F62*, 849–854.
7. Linden, A., Mayans, O., Meyer-Klaucke, W., Antranikian, G., and Wilmanns, M. (2003) Differential regulation of a hyperthermophilic α-amylase with a novel (Ca,Zn) two-metal center by zinc. *J. Biol. Chem. 278*, 9875–9884.
8. Ševcik, J., Hostinová, E., Solovicová, A., Gašperik, J., Dauter, Z., and Wilson, K. S. (2006) Structure of the complex of a yeast glucoamylase with acarbose reveals the presence of a raw starch binding site on the catalytic domain. *FEBS J. 273*, 2161–2171.
9. Vujicic-Žagar, A., and Dijkstra, B. W. (2006) Monoclinic crystal form of *Aspergillus niger* α-amylase in complex with maltose at 1.8 Å resolution. *Acta Crystallogr. F62*, 716–721.
10. Payan, F., and Qian, M. X. (2003) Crystal structure of the pig pancreatic α-amylase complexed with malto-oligosaccharides. *J. Protein Chem. 22*, 275–284.
11. Larson, S. B., Greenwood, A., Cascio, D., Day, J., and Mcpherson, A. (1994) Refined molecular-structure of pig pancreatic α-amylase at 2.1 Å resolution. *J. Mol. Biol. 235*, 1560–1584.
12. Qian, M. X., Haser, R., and Payan, F. (1995) Carbohydrate binding sites in a pancreatic α-amylase-substrate complex, derived from X-ray structure analysis at 2.1 Å resolution. *Protein Sci. 4*, 747–755.
13. Ragunath, C., Manuel, S. G., Venkataraman, V., Sait, H. B. R., Kasinathan, C., and Ramasubbu, N. (2008) Probing the role of aromatic residues at the secondary saccharide-binding sites of human salivary α-amylase in substrate hydrolysis and bacterial binding. *J. Mol. Biol. 384*, 1232–1248.
14. Kadziola, A., Søgaard, M., Svensson, B., and Haser, R. (1998) Molecular structure of a barley α-amylase-inhibitor complex: Implications for starch binding and catalysis. *J. Mol. Biol. 278*, 205–217.
15. Robert, X., Haser, R., Gottschalk, T. E., Ratajczak, F., Driguez, H., Svensson, B., and Aghajari, N. (2003) The structure of barley α-amylase isozyme 1 reveals a novel role of domain C in substrate recognition and binding: A pair of sugar tongs. *Structure 11*, 973–984.
16. Nielsen, M. M., Seo, E. S., Bozonnet, S., Aghajari, N., Robert, X., Haser, R., and Svensson, B. (2008) Multi-site substrate binding and interplay in barley α-amylase 1. *FEBS Lett. 582*, 2567–2571.
17. Bozonnet, S., Jensen, M. T., Nielsen, M. M., Aghajari, N., Jensen, M. H., Kramhøft, B., Willemoes, M., Tranier, S., Haser, R., and Svensson, B. (2007) The "pair of sugar tongs" site on the non-catalytic domain C of barley α-amylase participates in substrate binding and activity. *FEBS J. 274*, 5055–5067.
18. Robert, X., Haser, R., Mori, H., Svensson, B., and Aghajari, N. (2005) Oligosaccharide binding to barley α-amylase 1. *J. Biol. Chem. 280*, 32968–32978.
19. Tranier, S., Deville, K., Robert, X., Bozonnet, S., Haser, R., Svensson, B., and Aghajari, N. (2005) Insights into the "pair of sugar tongs" surface binding site in barley α-amylase isozymes and crystallization of appropriate sugar tongs mutants. *Biologia 60*, 37–46.
20. Kadziola, A., Abe, J., Svensson, B., and Haser, R. (1994) Crystal and molecular structure of barley α-amylase. *J. Mol. Biol. 239*, 104–121.
21. Bak-Jensen, K. S., André, G., Gottschalk, T. E., Paes, G., Tran, V., and Svensson, B. (2004) Tyrosine 105 and threonine 212 at outermost substrate binding subsites −6 and +4 control substrate specificity, oligosaccharide cleavage patterns, and multiple binding modes of barley α-amylase 1. *J. Biol. Chem. 279*, 10093–10102.
22. Kramhøft, B., Bak-Jensen, K. S., Mori, H., Juge, N., Nøhr, J., and Svensson, B. (2005) Involvement of individual subsites and secondary substrate binding sites in multiple attack on amylose by barley α-amylase. *Biochemistry 44*, 1824–1832.
23. Mori, H., Bak-Jensen, K. S., Gottschalk, T. E., Motawia, S. M., Damager, I., Møller, B. L., and Svensson, B. (2001) Modulation of activity and substrate binding modes by mutation of single and double subsites +1/+2 and −5/−6 of barley α-amylase 1. *Eur. J. Biochem. 268*, 6545–6558.
24. Mori, H., Bak-Jensen, K. S., and Svensson, B. (2002) Barley α-amylase Met53 situated at the high-affinity subsite −2 belongs to a substrate binding motif in the $\beta \rightarrow \alpha$ loop 2 of the catalytic $(\beta/\alpha)_8$-barrel and is critical for activity and substrate specificity. *Eur. J. Biochem. 269*, 5377–5390.
25. Kandra, L., Abou Hachem, M., Gyémánt, G., Kramhøft, B., and Svensson, B. (2006) Mapping of barley α-amylases and outer subsite mutants reveals dynamic high-affinity subsites and barriers in the long substrate binding cleft. *FEBS Lett. 580*, 5049–5053.
26. Albenne, C., Skov, L. K., Tran, V., Gajhede, M., Monsan, P., Remaud-Siméon, M., and André-Leroux, G. (2007) Towards the molecular understanding of glycogen elongation by amylosucrase. *Proteins 66*, 118–126.
27. Albenne, C., Skov, L. K., Mirza, O., Gajhede, M., Feller, G., D'Amico, S., André, G., Potocki-Véronèse, G., van der Veen, B. A., Monsan, P., and Remaud-Simeon, M. (2004) Molecular basis of the amylose-like polymer formation catalyzed by *Neisseria polysaccharea* amylosucrase. *J. Biol. Chem. 279*, 726–734.
28. Boraston, A. B., Bolam, D. N., Gilbert, H. J., and Davies, G. J. (2004) Carbohydrate-binding modules: Fine-tuning polysaccharide recognition. *Biochem. J. 382*, 769–781.
29. Machovic, M., and Janecek, S. (2006) Starch-binding domains in the post-genome era. *Cell. Mol. Life Sci. 63*, 1–15.
30. Machovic, M., Svensson, B., MacGregor, E. A., and Janecek, S. (2005) A new clan of CBM families based on bioinformatics of starch-binding domains from families CBM20 and CBM21. *FEBS J. 272*, 5497–5513.
31. Svensson, B., Jespersen, H., Sierks, M. R., and MacGregor, E. A. (1989) Sequence homology between putative raw-starch binding domains from different starch-degrading enzymes. *Biochem. J. 264*, 309–311.
32. Gibson, R. M., and Svensson, B. (1987) Identification of tryptophanyl residues involved in binding of carbohydrate ligands to barley α-amylase 2. *Carlsberg Res. Commun. 52*, 373–379.
33. Juge, N., Andersen, J. S., Tull, D., Roepstorff, P., and Svensson, B. (1996) Overexpression, purification, and characterization of recombinant barley α-amylases 1 and 2 secreted by the methylotrophic yeast *Pichia pastoris*. *Protein Expression Purif. 8*, 204–214.
34. Søgaard, M., Kadziola, A., Haser, R., and Svensson, B. (1993) Site-directed mutagenesis of histidine-93, aspartic acid-180, glutamic acid-205, histidine-290, and aspartic acid-291 at the active-site and tryptophan-279 at the raw starch binding-site in barley α-amylase 1. *J. Biol. Chem. 268*, 22480–22484.
35. Sambrook, J., and Russell, D. W. (2001) Molecular Cloning: A laboratory manual , Cold Spring Harbor Laboratory Press, Plainview, NY.
36. Søgaard, M., and Svensson, B. (1990) Expression of cDNAs encoding barley α-amylase 1 and α-amylase 2 in yeast and characterization of the secreted proteins. *Gene 94*, 173–179.
37. Kandra, L., Gyemant, G., Pal, M., Petro, M., Remenyik, J., and Liptak, A. (2001) Chemoenzymatic synthesis of 2-chloro-4-nitrophenyl β-maltoheptaoside acceptor-products using glycogen phosphorylase b. *Carbohydr. Res. 333*, 129–136.
38. Farkas, E., Janossy, L., Harangi, J., Kandra, L., and Liptak, A. (1997) Synthesis of chromogenic substrates of α-amylases on a cyclodextrin basis. *Carbohydr. Res. 303*, 407–415.
39. Gyémánt, G., Hovanszki, G., and Kandra, L. (2002) Subsite mapping of the binding region of α-amylases with a computer program. *Eur. J. Biochem. 269*, 5157–5162.
40. Nielsen, P. K., Bønsager, B. C., Berland, C. R., Sigurskjold, B. W., and Svensson, B. (2003) Kinetics and energetics of the binding between barley α-amylase/subtilisin inhibitor and barley α-amylase 2 analyzed by surface plasmon resonance and isothermal titration calorimetry. *Biochemistry 42*, 1478–1487.
41. Abou Hachem, M., Karlsson, E. N., Simpson, P. J., Linse, S., Sellers, P., Williamson, M. P., Jamieson, S. J., Gilbert, H. J., Bolam, D. N., and Holst, O. (2002) Calcium binding and thermostability of carbohydrate binding module CBM4-2 of Xyn10A from *Rhodothermus marinus*. *Biochemistry 41*, 5720–5729.

42. Gouet, P., Courcelle, E., Stuart, D. I., and Metoz, F. (1997) ESPript: Multiple sequence alignments in PostScript. *Bioinformatics 15*, 305–308.
43. Irwin, D., Shin, D. H., Zhang, S., Barr, B. K., Sakon, J., Karplus, P. A., and Wilson, D. B. (1998) Roles of the catalytic domain and two cellulose binding domains of *Thermomonospora fusca* E4 in cellulose hydrolysis. *J. Bacteriol. 180*, 1709–1714.
44. Allouch, J., Helbert, W., Henrissat, B., and Czjzek, M. (2004) Parallel substrate binding sites in a β-agarase suggest a novel mode of action on double-helical agarose. *Structure 12*, 623–632.
45. Ludwiczek, M. L., Heller, M., Kantner, T., and McIntosh, L. P. (2007) A secondary xylan-binding site enhances the catalytic activity of a single-domain family 11 glycoside hydrolase. *J. Mol. Biol. 373*, 337–354.
46. Vandermarliere, E., Bourgois, T. M., Rombouts, S., van Campenhout, S., Volckaert, G., Strelkov, S. V., Delcour, J. A., Rabijns, A., and Courtin, C. M. (2008) Crystallographic analysis shows substrate binding at the -3 to $+1$ active-site subsites and at the surface of glycoside hydrolase family 11 endo-1,4-β-xylanases. *Biochem. J. 410*, 71–79.
47. Mori, H. (2006) Identification and manipulation of subsite structure and starch granule binding site in plant α-amylase. *J. Appl. Glycosci. 53*, 51–56.
48. Oudjeriouat, N., Moreau, Y., Santimone, M., Svensson, B., Marchis-Mouren, G., and Desseaux, V. (2003) On the mechanism of α-amylase: Acarbose and cyclodextrin inhibition of barley amylase isozymes. *Eur. J. Biochem. 270*, 3871–3879.
49. Sorimachi, K., Le Gal-Coeffet, M. F., Williamson, G., Archer, D. B., and Williamson, M. P. (1997) Solution structure of the granular starch binding domain of *Aspergillus niger* glucoamylase bound to β-cyclodextrin. *Structure 5*, 647–661.
50. Sorimachi, K., Jacks, A. J., Le Gal-Coeffet, M. F., Williamson, G., Archer, D. B., and Williamson, M. P. (1996) Solution structure of the granular starch binding domain of glucoamylase from *Aspergillus niger* by nuclear magnetic resonance spectroscopy. *J. Mol. Biol. 259*, 970–987.
51. Giardina, T., Gunning, A. P., Juge, N., Faulds, C. B., Furniss, C. S. M., Svensson, B., Morris, V. J., and Williamson, G. (2001) Both binding sites of the starch-binding domain of *Aspergillus niger* glucoamylase are essential for inducing a conformational change in amylose. *J. Mol. Biol. 313*, 1149–1159.
52. Williamson, M. P., Le Gal-Coeffet, M. F., Sorimachi, K., Furniss, C. S., Archer, D. B., and Williamson, G. (1997) Function of conserved tryptophans in the *Aspergillus niger* glucoamylase 1 starch binding domain. *Biochemistry 36*, 7535–7539.
53. Penninga, D., van der Veen, B. A., Knegtel, R. M. A., van Hijum, S. A. F. T., Rozeboom, H. J., Kalk, K. H., Dijkstra, B. W., and Dijkhuizen, L. (1996) The raw starch binding domain of cyclodextrin glycosyltransferase from *Bacillus circulans* strain 251. *J. Biol. Chem. 271*, 32777–32784.
54. Southall, S. M., Simpson, P. J., Gilbert, H. J., Williamson, G., and Williamson, M. P. (1999) The starch-binding domain from glucoamylase disrupts the structure of starch. *FEBS Lett. 447*, 58–60.
55. Juge, N., Nøhr, J., Le Gal-Coeffet, M. F., Kramhøft, B., Furniss, C. S. M., Planchot, V., Archer, D. B., Williamson, G., and Svensson, B. (2006) The activity of barley α-amylase on starch granules is enchanced by fusion of a starch binding domain from *Aspergillus niger* glucoamylase. *Biochim. Biophys. Acta 1764*, 275–284.
56. Stam, M. R., Danchin, E. G. J., Rancurel, C., Coutinho, P. M., and Henrissat, B. (2006) Dividing the large glycoside hydrolase family 13 into subfamilies: Towards improved functional annotations of α-amylase-related proteins. *Protein Eng., Des. Sel. 19*, 555–562.